

FALCON: Resolving Visual Redundancy and Fragmentation in High-resolution Multimodal Large Language Models via Visual Registers

Renshan Zhang¹, Rui Shao^{1†}, Gongwei Chen¹, Kaiwen Zhou², Weili Guan¹, Liqiang Nie^{1†}

¹Harbin Institute of Technology, Shenzhen ²Huawei Noah’s Ark Lab

zhangrenshan@stu.hit.edu.cn shaorui@hit.edu.cn

chengongwei@hit.edu.cn nieliqiang@gmail.com

<https://github.com/JiuTian-VL/JiuTian-FALCON>

Abstract

The incorporation of high-resolution visual input equips multimodal large language models (MLLMs) with enhanced visual perception capabilities for real-world tasks. However, most existing high-resolution MLLMs rely on a cropping-based approach to process images, which leads to fragmented visual encoding and a sharp increase in redundant tokens. To tackle these issues, we propose the **FALCON** model. **FALCON** introduces a novel **visual register** technique to simultaneously: **1) Eliminate redundant tokens at the stage of visual encoding.** To directly address the visual redundancy present in the output of vision encoder, we propose a Register-based Representation Compacting (**ReCompact**) mechanism. This mechanism introduces a set of learnable visual registers designed to adaptively aggregate essential information while discarding redundancy. It enables the encoder to produce a more compact visual representation with a minimal number of output tokens, thus eliminating the need for an additional compression module. **2) Ensure continuity in visual encoding.** To address the potential encoding errors caused by fragmented visual inputs, we develop a Register Interactive Attention (**ReAtten**) module. This module facilitates effective and efficient information exchange across sub-images by enabling interactions between visual registers. It ensures the continuity of visual semantics throughout the encoding. We conduct comprehensive experiments with **FALCON** on high-resolution benchmarks across a wide range of scenarios. **FALCON** demonstrates superior performance with a remarkable **9-fold** and **16-fold** reduction in visual tokens.

1. Introduction

Recently, multimodal large language models (MLLMs) [3, 8, 29, 31, 64, 65] have made significant advancements in

[†]Corresponding authors

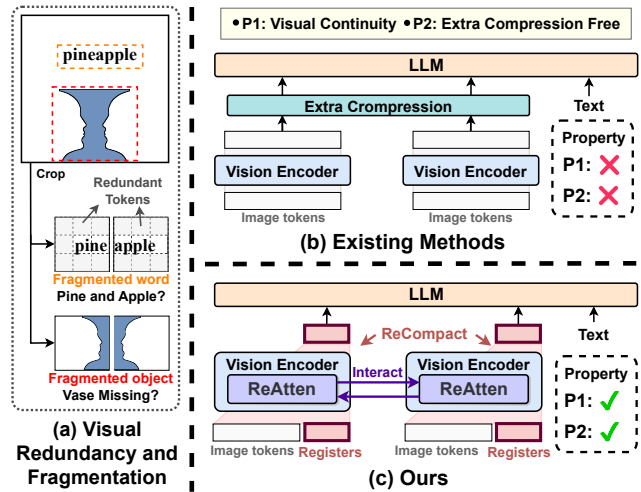


Figure 1. Comparison between existing high-resolution MLLMs and FALCON. FALCON eliminates visual redundancy and ensures the continuity of high-resolution encoding through the use of ReCompact and ReAtten mechanisms.

performing vision-language tasks, facilitating more natural human-machine interactions. Early MLLMs [8, 31, 64] typically processed images at a fixed low resolution, such as 224×224. This limited their capabilities in many real-world applications that require high-resolution input. To equip MLLMs with high-resolution visual perception, recent advancements [14, 17, 32, 63, 69] have introduced a cropping-based high-resolution processing method. Specifically, As shown in Fig. 1(b), this approach crops high-resolution images into multiple non-overlapping sub-images that match the pre-trained resolution of the encoder. Each sub-image is processed independently by the vision encoder. Then the resulting visual features are concatenated and fed into the large language model (LLM).

Although effective, cropping-based methods still face issues of: **1) Visual Redundancy.** The number of visual tokens grows dramatically with increasing resolution. While

this enriches the visual details, it also leads to an increase in redundant tokens. These redundant tokens significantly increase the computational burden on LLM and interfere with the processing of visual information [68]. To address these issues, as illustrated in Fig. 1(b), existing methods typically rely on additional compression techniques. Representative approaches include combining learnable queries with cross-attention [2, 28, 65] or simply employing pooling layers [48, 60]. However, these methods either demand substantial training resources or fail to fully address redundancy. **2) Visual Fragmentation.** Cropping an image into multiple non-overlapping sub-images may disrupt visual semantics and potentially lead to encoding errors. As shown in Fig. 1(a), in an OCR task, the word “pineapple” may be incorrectly segmented into “pine” and “apple”, causing the LLM to misinterpret the word. Similarly, fragmentation can also hinder the identification of objects. For example, the “rubin vase” pattern illustrated in Fig. 1(a) depicts both a vase and two faces simultaneously. However, the fragmentation could lead to the vase being unrecognizable.

To address these issues, as shown in Fig. 1(c), we propose the **FALCON** model. FALCON introduces a novel **visual register** technique to simultaneously: **1) Eliminate redundant tokens during visual encoding.** To eliminate redundancy directly at the stage of visual encoding, we propose a novel Register-based Representation Compacting (**ReCompact**) mechanism. This mechanism introduces a set of learnable visual registers as additional inputs to the vision encoder. The registers are designed to adaptively aggregate essential information from image tokens and discard redundant content. Then the outputs corresponding to the visual registers are considered as a non-redundant visual representation, serving as the compact input for the LLM instead of a large number of image tokens. This mechanism enables the vision encoder to convey comprehensive visual information in a compact representation using minimal tokens, thus removing the need for an additional compression module. **2) Ensure continuity in visual encoding.** To avoid the potential encoding errors caused by fragmented visual inputs, we develop a novel Register Interactive Attention (**ReAtten**) module. This module leverages the compact and comprehensive representation produced by visual registers to facilitate information exchange across sub-images. It gathers visual registers from different sub-images and employs a specialized cross-ViT attention module to enable interactions among them. Such interaction enables thorough information exchange across the entire image, thus ensuring visual continuity throughout the encoding process. Additionally, the compactness of the visual registers further enhances the efficiency of these interactions. Consequently, this module provides LLMs with a reliable foundation to accurately interpret visual content and reduce hallucinations.

We summarize our main contributions as follows:

- To address the issue of visual redundancy directly at the encoding phase, we introduce the Register-base Representation Compacting (ReCompact) mechanism. This mechanism enables vision encoder to capture rich visual information using only a minimal number of tokens, effectively eliminating redundancy and obviating the need for additional compression modules.
- To address the issue of visual fragmentation caused by image cropping, we propose the register interactive attention (ReAtten) module. This module ensures the semantic continuity of high-resolution visual encoding in an efficient and effective manner.
- We introduce FALCON, a model that leverages the proposed visual register technique. Comprehensive evaluations on high-resolution visual understanding benchmarks highlight the superiority of FALCON. Notably, FALCON achieves exceptional results with a remarkable reduction in visual tokens by 9× and 16×.

2. Related Work

2.1. Multimodal Large Language Models

Research on MLLMs [2, 3, 29, 47, 64, 65] has made significant strides in recent years. By incorporating image inputs into pretrained LLMs [7, 55, 56], MLLMs demonstrate strong capabilities across various vision-language tasks. Typically, these models use a pretrained vision encoder [45, 66] to transform input images into a set of visual tokens. These tokens are then projected into the input space of the LLM through a projection module (e.g., MLP [29, 31], QFormer [8] and Abstractor [65]) and processed alongside text inputs. Building on the progress of MLLMs, recent studies have started to explore their applications in practical tasks such as document understanding [14, 62], agents [27], and autonomous driving [59]. Despite these advances, MLLMs still struggle with the fixed low resolution of pretrained image encoders, which can limit their effectiveness in handling high-resolution images.

2.2. High-resolution MLLMs

To address the limitation of MLLMs in handling only low-resolution visual inputs, early studies attempted to either directly incorporate vision encoders that were pre-trained on higher-resolution images [35, 38], or to improve the resolution of pre-trained encoders through additional training [2, 65]. While achieving some progress, they still remain restricted by the fixed resolutions. To accommodate the varying resolutions and aspect ratios, cropping-based techniques have been widely adopted in recent works [14, 17, 32, 63, 69]. However, these approaches still face challenges related to visual redundancy and fragmentation.

To mitigate the issue of redundancy, existing models typically require an additional compression module. For ex-

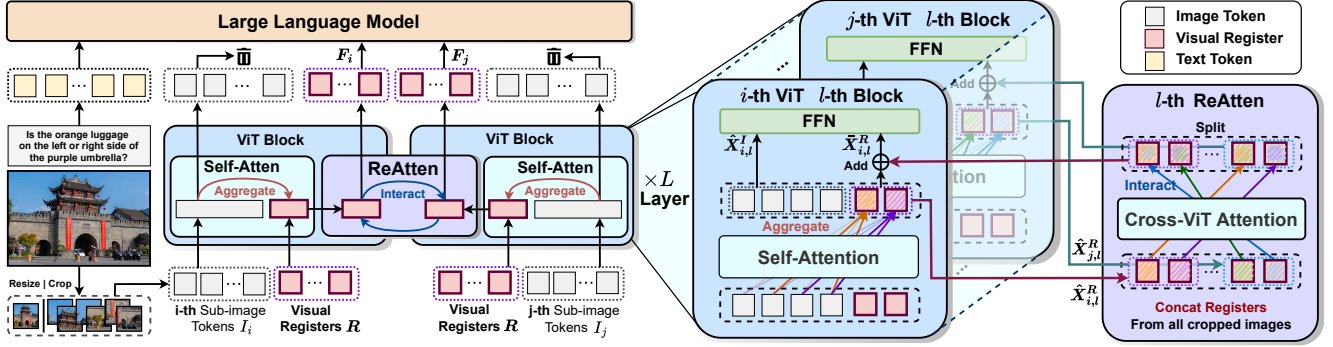


Figure 2. Overall framework of the proposed FALCON. The model introduces a set of learnable visual registers, which are fed into the ViT along with the image tokens from each sub-image. During the visual encoding, the ReCompact mechanism enables information from the image tokens to be aggregated into the visual registers, while the proposed ReAtten facilitates information exchange among the visual registers across different sub-images. Ultimately, these visual registers provide a compact visual representation as input to the LLM.

ample, Abstractor-like modules utilizing learnable queries combined with cross-attention are widely adopted [2, 28, 32, 63, 65]. These modules typically require pretraining on massive amounts of data, which diminishes their practical efficacy. In contrast, some approaches use pooling layers [48, 60] or convolutional layers [14, 35]. Though resource-efficient, they often fail to address the issue of redundancy. In this work, we present an initial exploration to directly eliminate redundancy during the visual encoding phase, thereby removing the need for additional compression. To address the issue of fragmentation, several concurrent studies also make preliminary investigation. TextMonkey [32] uses Shifted Window Attention [34] to exchange information between sub-images. But the exchange is still limited to local regions. MiniMonkey [16] proposed a Complementary Image Pyramid strategy to generate complementary cropping schemes. However, this strategy inevitably encodes the same visual content multiple times, further exacerbating visual redundancy. In this work, we propose the ReAtten module to facilitate continuous visual encoding through the interaction among visual registers.

3. FALCON

The overall framework of FALCON is illustrated in Fig. 2. The method begins with shape-adaptive cropping [63], where the image is cropped into multiple non-overlapping sub-images, each matching the resolution of the pre-trained vision encoder. Additionally, a resized version of the full image is used to supplement global layout information. To directly eliminate redundancy during visual encoding, we propose Register-based Representation Compacting (ReCompact) mechanism. This mechanism introduces a set of learnable visual registers, which are paired with image tokens from each sub-image and fed into the vision encoder to capture rich visual information. To ensure the continuity of visual semantics throughout the encoding, a novel Regis-

ter Interactive Attention (ReAtten) module is integrated into the Vision Transformer (ViT) [10] to facilitate information exchange between sub-images via the visual registers. Finally, the compact visual representations produced by the visual registers are processed through a simple MLP module before being fed into the LLM for further analysis.

3.1. Mitigating Visual Redundancy via ReCompact

Existing MLLMs typically use a ViT-based vision encoder, such as CLIP [45]. For an input image of size $H \times W$, it is patchified into multiple $P \times P$ patches. Each patch is treated as an individual image token, resulting in $N = \frac{H}{P} \times \frac{W}{P}$ tokens, denoted as $I = \{i_1, \dots, i_N\}$. In most current MLLMs, output features corresponding to all image tokens are usually preserved in their entirety. However, when high-resolution images are included, the number of image tokens increases dramatically, placing a substantial burden on the computational resources of LLMs. Consequently, most high-resolution MLLMs necessitate an additional compression module, which can be resource-inefficient. Previous research has shown that most image tokens contain only localized information from their surrounding areas [9]. It suggests that a significant portion of these tokens may be redundant, particularly those originating from background regions. This observation motivates us to directly eliminate redundancy in the output of the vision encoder, thereby reducing the number of visual tokens and avoiding the need for an additional compression module.

To achieve this, we propose a novel Register-based Representation Compacting (**ReCompact**) mechanism. This mechanism employs a set of visual registers to aggregate essential information from image tokens, resulting in a more compact visual representation. Specifically, as shown in Fig. 2, we introduce a set of learnable visual registers, denoted by $R = \{r_1, \dots, r_M\}$, where M represents the number of visual registers, and $M \ll N$. Given a single input image, the image tokens are concatenated with

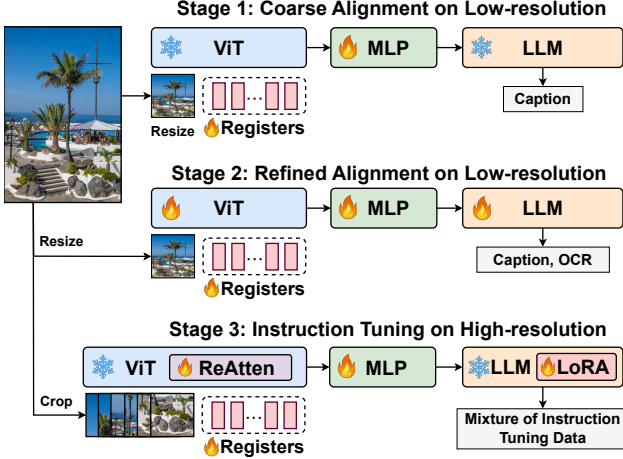


Figure 3. The progressive training pipeline. **Stage 1:** Pretrain visual registers and MLP on low-resolution for coarse alignment. **Stage 2:** Tune all parameters with caption and OCR data on low-resolution for refined alignment. **Stage 3:** Integrate high-resolution input and ReAtten module for instruction tuning.

visual registers to create a new input for ViT, represented as $V = \text{Concat}(I, R) = \{i_1, \dots, i_N, r_1, \dots, r_M\}$. During visual encoding, the self-attention mechanism in ViT enables the visual register to adaptively aggregate important information from image tokens while discarding redundant content. Denote $X_{k,l} \in \mathcal{R}^{(N+M) \times D}$ as the input hidden states of the k -th sub-image at the l -th layer, where D is the dimensionality. The self-attention is formulated as:

$$\hat{X}_{k,l} = \text{Self-Atten}(X_{k,l}) = \text{Softmax}\left(\frac{X_{k,l}X_{k,l}^T}{\sqrt{D_{key}}}\right)X_{k,l} \quad (1)$$

Notably, we do not apply any attention masks for specific constraints. Our experiments show that pretraining on a modest amount of data is sufficient to effectively adapt the pretrained ViT to the proposed ReCompact, enabling it to aggregate essential information within the visual registers. After visual encoding, The output features corresponding to the visual registers, denoted as $F = \{f_1, \dots, f_M\}$, are then used as the visual representation of the image and fed into the LLM for various vision-language tasks.

To further adapt the ReCompact mechanism for cropping-based high-resolution image perception, we share the same set of visual registers as input for different sub-images. The input for the k -th sub-image is formulated as $V_k = \text{Concat}(I_k, R)$, where $k = 1, 2, \dots, N_c$ and N_c denotes the total number of sub-images. After encoding, the outputs of the visual registers for all sub-images are concatenated, yielding $F_{hr} = \text{Concat}(F_1, F_2, \dots, F_{N_c})$, which serves as the input to the LLM. The ReCompact mechanism enables the vision encoder to represent rich visual information using only a minimal number of M tokens per sub-image, which significantly reduces the visual redun-

dancy and eliminates the need for additional compression.

The proposed ReCompact mechanism differs significantly from widely used Abstractor-like modules [2, 8, 28, 32, 63, 65]. While both share the goal of generating compact and non-redundant visual representations, the ReCompact shows notable advantages. Abstractor-like modules typically consist of multiple stacked Transformer [57] blocks, serving as an additional compression module between the vision encoder and the LLM. These modules use a set of query tokens to extract information from output image tokens through cross-attention in each block. In contrast, based on the observation that a well-pretrained ViT can naturally gather global information into some specific tokens through self-attention [9], ReCompact directly adopts the pretrained ViT to aggregate information into a set of specified register tokens. This design offers ReCompact several strengths in terms of: **1) Parameter Efficiency.** Introducing abstractor-like modules significantly increases the number of parameters, whereas ReCompact avoids this issue by directly adapting the pretrained ViT. This mitigates the hardware burden in terms of both time and space. **2) Training Efficiency.** The substantial number of randomly initialized parameters in Abstractor-like modules requires extensive data for pretraining. For instance, Qformer [23], Abstractor [65], and Resampler [2] use large corpora of 129M, 400M, and 1.4B samples, respectively. In contrast, by leveraging well-pretrained ViT parameters, ReCompact requires fewer than 2M samples for adaptation. The ablation results in Fig. 4 further demonstrate these advantages.

3.2. Ensuring Visual Continuity via ReAtten

When using the cropping-based high-resolution image encoding method, each sub-image is independently encoded by the vision encoder. This process can disrupt semantic coherence and result in the misrepresentation of visual concepts. To preserve the continuity of visual semantics, it is crucial to enable information exchange between sub-images during encoding. A naive approach would be to directly concatenate the image features from all sub-images and apply self-attention. However, the quadratic computational complexity makes this approach impractical. In Sec. 3.1, we introduced the ReCompact mechanism, where the visual registers effectively aggregate rich visual information while discarding redundancy during visual encoding, allowing them to serve as compact yet comprehensive image representations. Consequently, interactions between visual registers can naturally facilitate sufficient information exchange across different sub-images in an efficient manner.

To enable information exchange between visual registers across different sub-images, we introduce a novel Register Interactive Attention (**ReAtten**) module. As shown in Fig. 2, the ReAtten module is integrated into each of the L layers of the ViT. After the self-attention process in Eq.

(1), we acquire $\hat{X}_{k,l} = \{\hat{X}_{k,l}^I, \hat{X}_{k,l}^R\}$, where $\hat{X}^I \in \mathcal{R}^{N \times D}$ and $\hat{X}^R \in \mathcal{R}^{M \times D}$ represent the hidden states corresponding to image tokens and visual registers, respectively. The states of the visual registers from different sub-images are concatenated to form $\hat{X}_l^R = \text{Concat}(\{\hat{X}_{k,l}^R\}_{k=1}^{N_c}) \in \mathcal{R}^{M \cdot N_c \times D}$. Then these concatenated registers are processed via ReAtten to enable information exchange across sub-images, which can be formulated as:

$$\bar{X}_l^R = \text{ReAtten}(\hat{X}_l^R) = \hat{X}_l^R + \text{Cross-ViT-Atten}(\hat{X}_l^R) \quad (2)$$

where Cross-ViT-Atten is implemented as a self-attention layer. Once the information exchange is completed, the registers and image tokens from a same sub-image are concatenated and then passed into the feedforward network (FFN) for transformation, yielding the output of the l -th layer:

$$X_{k,l+1} = \text{FFN}(\text{Concat}(\hat{X}_{k,l}^I, \bar{X}_{k,l}^R)) \quad (3)$$

By integrating ReAtten into each layer of the ViT model, FALCON enables effective information exchange between cropped sub-images through visual registers, thereby ensuring semantic continuity of the high-resolution image throughout the visual encoding process.

3.3. Learning Expressive Visual Representation via Progressive Training Pipeline

To empower the ReCompact mechanism with the capability to capture rich visual patterns and to enable smoother initialization of the ReAtten module under high-resolution conditions, we develop a specialized progressive training pipeline. As illustrated in Fig. 3, this pipeline progressively transitions from low to high resolution across three stages.

Stage 1: Coarse Alignment on Low-resolution. Since both the visual registers and the MLP module are randomly initialized, in stage 1, we aim to initially achieve a coarse alignment between the pretrained vision encoder and the LLM. To facilitate this, we begin by using low-resolution images as inputs, which are directly resized to match the pretraining resolution of the vision encoder. We then train the visual registers and the MLP using image caption data, while keeping both the vision encoder and the LLM frozen.

Stage 2: Refined Alignment on Low-resolution. To better adapt the pre-trained vision encoder to our newly introduced ReCompact mechanism, in stage 2, we unfreeze all model parameters to enable a more refined alignment. To enhance the capacity of the visual register to capture detailed and comprehensive visual information, we employ high-quality, extended captions that are rich in fine-grained details, along with a diverse set of full-document OCR data. Additionally, to ensure resource efficiency, we continue to use low-resolution image inputs. By combining these low-resolution inputs with the compact visual representations

produced by the ReCompact mechanism, this approach facilitates efficient full parameter fine-tuning.

Stage 3: Instruction Tuning on High-resolution. To adapt the well-aligned visual register for a wide range of real-world vision-language tasks, in stage 3, we transition the model to process high-resolution image inputs. In this stage, we employ the cropping-based approach to empower the model with enhanced capability of high-resolution perception. Additionally, the proposed ReAtten module is integrated to address visual fragmentation caused by cropping-based high-resolution image encoding. To improve instruction-following performance, the training process utilizes a mixture of instruction-tuning datasets covering various tasks, such as VQA, document understanding, and grounding. To maintain resource efficiency during high-resolution training, the parameters of the vision encoder and the LLM are kept frozen, while only the LoRA parameters of the LLM and the remaining parameters are trainable. Notably, to facilitate a smoother initialization for the newly introduced ReAtten modules, we initialize parameters of each ReAtten module with the ViT self-attention parameters at the corresponding depth.

4. Experiments

We implement FALCON on pretrained LLMs of two different sizes, resulting in FALCON-7B and FALCON-3B. The numbers of visual registers for FALCON-7B and FALCON-3B are set to 64 and 36, respectively, achieving remarkable visual token compression rates of $9\times$ and $16\times$. For detailed information regarding the architecture, datasets and training settings, please refer to the **Appendix**.

4.1. Experimental Results

We evaluate FALCON using the recently proposed MME-RealWorld [70] benchmark, a comprehensive and large-scale benchmark specifically designed to assess the high-resolution understanding capabilities of MLLMs. MME-RealWorld comprises 13,366 high-resolution images with an average resolution of $2,000 \times 1,500$ pixels, spanning five domains: OCR in the wild, Remote Sensing, Diagrams and Tables, Monitoring, and Autonomous Driving. This benchmark is well-suited for evaluating the practical high-resolution understanding capabilities of MLLMs.

As shown in Tab. 1, FALCON-7B and FALCON-3B significantly outperform other advanced MLLMs in both perception and reasoning tasks. FALCON-7B achieves state-of-the-art performance with only **64** tokens per sub-image, resulting in a remarkable visual compression rate of 9 times. Furthermore, FALCON-3B achieves the second-best performance while using significantly fewer parameters of 3B and an even more impressive count of just **36** tokens per sub-image. In addition, even compared to models trained on much larger datasets, FALCON remains highly compet-

Table 1. Evaluation on MME-RealWorld Benchmark. “OCR”, “RS”, “DT”, “MO”, and “AD” stand for OCR in the Wild, Remote Sensing, Diagram and Table, Monitoring, and Autonomous Driving, respectively. “Avg” denotes the weighted average accuracy across all samples, while “Avg-C” denotes the weighted average accuracy across different domains. “Size” indicates the image resolution supported by the model, where $\times n$ signifies a cropping-based high-resolution processing approach with up to n sub-images. “Token” denotes the number of visual tokens after compression. † For models utilizing hybrid vision encoders, “Size” and “Token” represent the setting of encoder with most tokens. We gray out the models that are either closed-source or trained on a corpus that is at least **three times** larger than ours. Among these, lighter gray denotes scores below ours. The underline indicates that top-3 performance is achieved. Notably, FALCON-7B achieves state-of-the-art performance with just **64** tokens per sub-image, surpassing even some advanced closed-source commercial models. Meanwhile, FALCON-3B also demonstrates impressive results, achieving a ranking just below FALCON-7B, despite having significantly fewer parameters and visual tokens—only **36** tokens per sub-image.

Type	Method	Size ^v	Token ^c	Perception					Reasoning							
	Task Split			OCR	RS	DT	MO	AD	Avg	Avg-C	OCR	DT	MO	AD	Avg	Avg-C
Training Data \$< 5M\$	MiniGPT-v2 [5]	448 ²	256	39.0	23.3	20.4	19.3	26.0	26.9	25.6	30.0	20.4	16.9	23.7	23.0	22.7
	LLaVA1.5-13B [29]	336 ²	576	44.1	23.3	20.2	20.5	26.1	28.4	26.8	30.2	20.8	27.5	24.8	25.5	25.8
	ShareGPT4V-13B [6]	336 ²	576	44.6	23.1	20.2	19.3	26.1	28.4	26.6	26.0	20.8	27.3	24.6	24.6	24.7
	TextMonkey [32]	448 ² \times 4	256 \times 4	37.3	11.7	5.9	16.1	14.3	18.2	17.1	30.4	2.2	4.4	20.0	16.0	14.3
	LLaVA-Next-Qwen72B [30]	336 ² \times 4	576 \times 4	37.1	29.1	27.7	29.4	18.0	29.0	28.3	17.2	34.2	27.3	29.7	27.9	27.1
	LLaVA-Next-llama3 [30]	336 ² \times 4	576 \times 4	47.9	25.4	26.6	19.5	18.7	30.1	27.6	55.2	23.4	21.1	30.7	32.1	32.6
	Mini-Gemini-7B-HD† [26]	336 ² \times 4	576	42.0	31.3	22.3	34.2	24.8	31.1	30.9	35.4	24.6	25.9	23.3	26.1	27.3
	DeepSeek-VL† [35]	1024 ²	576	49.6	25.5	23.4	27.0	33.4	33.1	31.8	45.2	23.8	16.7	27.3	28.0	28.3
	mPLUG-DocOwl 1.5 [14]	448 ² \times 9	256 \times 9	51.2	23.7	29.3	25.0	28.3	33.7	31.5	42.6	19.8	20.5	26.0	26.9	27.2
	Monkey [28]	448 ² \times 4	256 \times 4	54.6	25.0	32.5	28.0	29.7	36.3	34.0	27.2	20.8	27.3	33.0	28.8	27.1
	FALCON-3B	336 ² \times 16	36 \times 16	<u>57.3</u>	<u>35.7</u>	<u>34.5</u>	<u>31.6</u>	<u>33.1</u>	<u>40.5</u>	<u>38.4</u>	<u>48.2</u>	29.8	19.9	31.7	<u>32.2</u>	<u>32.4</u>
FALCON-7B	336 ² \times 16	64 \times 16	60.1	43.5	41.4	34.4	39.5	45.9	43.8	<u>50.8</u>	29.8	32.9	31.7	34.8	36.2	
Training Data \$> 10M\$	Qwen-VL-Chat [2]	448 ²	256	32.4	15.1	15.6	22.1	15.1	20.8	20.1	28.6	13.6	16.5	24.6	22.0	20.8
	Cambrian-1-8B† [54]	1024 ²	576	58.7	40.1	32.7	47.7	38.5	43.8	43.5	53.2	27.4	42.4	30.7	36.2	38.4
	CogVLM2-llama3-Chat [13]	1344 ²	2304	70.0	28.8	47.5	33.7	30.2	45.8	42.0	54.0	32.8	41.2	31.2	37.3	39.8
	MiniCPM-V 2.5 [61]	448 ² \times 9	96 \times 9	66.8	27.7	52.8	38.7	34.2	47.4	44.0	44.0	31.8	37.0	31.0	34.5	36.0
	IXC2.5 [67]	560 ² \times 24	400 \times 24	69.3	36.1	63.9	39.5	33.6	52.5	48.5	53.4	41.0	17.7	30.0	33.9	35.5
Closed-source	GPT-4o-mini	-	-	62.5	6.7	44.2	26.5	24.2	37.1	32.8	47.0	39.8	25.8	26.8	32.5	34.9
	Gemini-1.5-pro [53]	-	-	67.6	14.0	39.9	31.1	26.6	39.6	35.9	52.7	33.2	28.3	19.2	29.2	33.4
	GPT-4o	-	-	77.7	28.9	46.7	33.9	22.4	46.4	41.9	61.4	44.8	36.5	26.4	37.6	42.3
	Claude 3.5 Sonnet	-	-	72.5	25.7	67.4	32.2	40.8	52.9	47.7	61.9	61.2	41.8	31.9	44.1	49.2

itive. Specifically, FALCON-7B outperforms CogVLM2-llama3-Chat [13] in average scores on the perception task, which uses over 1 billion samples for training. It also surpasses MiniCPM-V 2.5 [61] and IXC2.5 [67] in average scores on the reasoning tasks, which utilize hundreds of millions of samples. FALCON-7B also exceeds all models trained on large corpora in several sub-tasks, including remote sensing and autonomous driving. Notably, FALCON achieves higher average scores in both perception and reasoning tasks compared to two advanced commercial models, GPT-4o-mini and Gemini-1.5-pro [53], with FALCON-7B notably outperforming all commercial models in the sub-tasks of remote sensing and monitoring. These results demonstrate that the ReCompact and ReAtten technique proposed by FALCON effectively eliminate visual redundancy and ensure visual continuity, allowing comprehensive and detailed visual information to be conveyed with a highly compact visual representation.

To further assess FALCON’s capabilities in high-

resolution understanding, we conduct evaluations on three additional high-resolution benchmarks: V* [58], DocVQA [41], and TextVQA [50]. V* encompasses tasks related to attribute recognition and spatial reasoning in natural scenes, focusing on evaluating the models’ capabilities for detailed visual analysis. DocVQA challenges models to comprehend text-dense, high-resolution document images, while TextVQA evaluates the ability to recognize small text in real-world scenes. As shown in Tab. 2, FALCON demonstrates superior performance across all these benchmarks.

To evaluate the performance of FALCON across a broader range of domains, we further select three popular benchmarks: POPE [25], ScienceQA [37], and MM-Bench [33]. These benchmarks specifically assess models’ capabilities in hallucination, scientific reasoning, and comprehensive ability, respectively. As shown in Tab. 3, FALCON-7B and FALCON-3B achieve state-of-the-art and second-best performance across the three benchmarks, respectively. These results demonstrate that FALCON excels

Table 2. Evaluations on diverse high-resolution Benchmarks. “ V^*_{Avg} ” represents the weighted average score for the two sub-tasks in the V^* benchmark. * The TextVQA score of Monkey [28] is sourced from [16]. † denotes OCR inputs are utilized.

Model	V^*_{Avg}	DocVQA	TextVQA
Low-resolution MLLMs			
Qwen-VL [2]	-	65.1	63.8
InstructBLIP [8]	34.0	4.5	50.7
LLaVA-v1.5-7B [31]	48.7	8.5	58.2†
mPLUG-Owl2 [65]	-	17.9	58.2†
High-resolution MLLMs			
UReader [63]	-	65.4	57.6
Monkey [28]	-	66.5	64.3*
LlaVA-FlexAttn [24]	54.4	-	48.9
S2-Wrapper-7B [48]	55.5	-	61.0
LLaVA-Next-Vicuna7B [30]	61.8	-	64.9
SliME-7B [69]	-	-	64.4
FALCON-3B	55.0	68.0	64.1
FALCON-7B	63.3	<u>67.9</u>	65.8

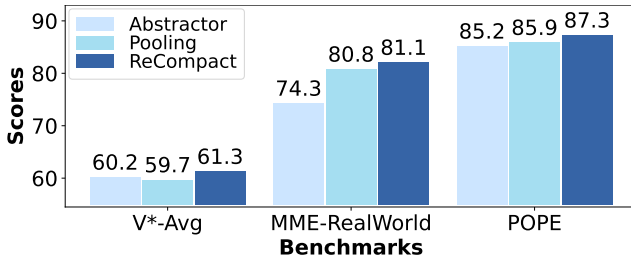


Figure 4. Comparison of different compression methods. We report the sum of the “Avg-C” scores for the perception and reasoning tasks in MME-RealWorld. The superior performance demonstrates that ReCompact effectively eliminates redundancy and produces a more expressive and compact visual representation.

not only in high-resolution understanding but also exhibits superior capabilities across a wide range of tasks.

4.2. Ablation Study

We perform extensive ablation studies to validate the effectiveness of the proposed ReCompact and ReAtten. All experiments are conducted with 64 visual registers with up to 9 sub-images. In stage 3, a subset of 800k samples is used.

Effectiveness of ReCompact mechanism. To verify the advantages of the proposed ReCompact mechanism in reducing visual redundancy and compressing visual representations during the visual encoding phase, we compare the ReCompact with other commonly used compression methods. This includes pooling layers [48, 60] and the Abstractor [65]. The latter serves as a representative module of the query token combined with cross-attention.

As shown in Fig. 4, ReCompact demonstrates superior performance compared to both pooling and Abstractor. These results indicate that ReCompact effectively eliminates visual redundancy and produces a more expressive compact visual representation. In contrast, we argue that

Table 3. Evaluation on benchmarks across diverse domains. The POPE, SQA, and MMBench benchmarks are used to assess hallucination, scientific reasoning, and overall abilities, respectively. MMBench results are taken from the OpenCompass Leaderboard, with * indicating results sourced from respective papers.

Model	SQA	POPE	MMB
Low-Resolution MLLMs			
Qwen-VL [2]	67.1	-	41.6
InstructBLIP [8]	63.1	78.9	38.4
LlaVA-v1.5-7B [31]	66.8	85.9	62.8
mPLUG-Owl2 [65]	68.7	85.8	63.5
High-Resolution MLLMs			
Monkey [28]	69.4	-	57.4
LlaVA-FlexAttn [24]	-	85.9	65.7*
S2-Wrapper-7B [48]	-	-	66.2*
LLaVA-Next-Vicuna7B [30]	70.1	86.5	66.5
SliME-7B [69]	76.8	85.4	63.1
FALCON-3B	84.4	87.0	73.3
FALCON-7B	85.5	87.3	73.6

Table 4. Comparison of different methods for maintaining visual continuity. The “Baseline” model refers to a condition where no specific methods are applied to preserve visual continuity. We report the “Avg-C” score for MME-RealWorld. The results show that the ReAtten module more effectively addresses the issue of visual fragmentation compared to other methods, thereby improving overall performance and reducing hallucinations.

Method	V^*_{Avg}	MME-RealWorld		POPE
		Perception	Reasoning	
Baseline	51.3	38.2	35.6	85.7
CIP [16]	50.3	38.4	37.2	86.3
W-Attn [32]	60.2	41.0	38.1	86.4
ReAtten	61.3	42.1	39.0	87.3

the pooling layer merely reduces the number of tokens by merging adjacent ones, failing to eliminate redundancy that interferes with the LLM’s understanding of visual content. Additionally, although Abstractor uses significantly more parameters, its performance is generally lower than that of pooling and ReCompact. This result suggests that even millions of samples may be insufficient for fully training Abstractor, which diminishes their practical efficacy.

Effectiveness of ReAtten Module. To validate the advantage of the proposed ReAtten Module, we compare ReAtten with other contemporary methods, including the Shifted Window Attention (W-Attn) [34] adopted by TextMonkey [32] and the Complementary Image Pyramid (CIP) introduced by MiniMonkey [16].

As shown in Tab. 4, the model incorporating ReAtten achieves significant improvements over the baseline across all benchmarks and demonstrates superiority compared to other methods. These results indicate that the ReAtten module effectively enhances the ability of the model in high-resolution perception and mitigates hallucinations by ad-

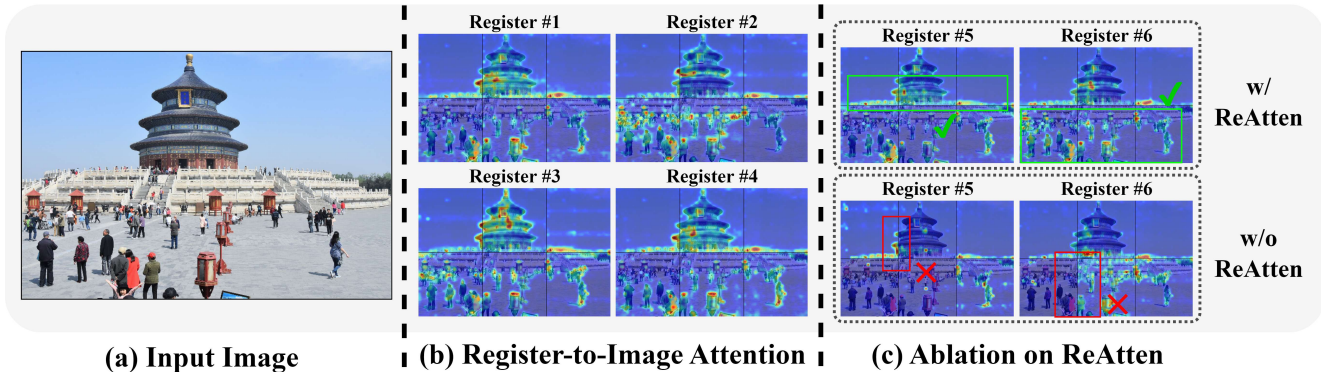


Figure 5. Visualization of the register-to-image attention map. We randomly select several visual registers and extract the attention scores that each register assigns to image tokens in the ViT model. We then create a heatmap and overlay it on the input image to visualize the attention patterns. The results in (b) shows that each visual register focuses on specific parts of the image, capturing rich visual patterns. Meanwhile, registers pay minimal attention to background areas, effectively avoiding the inclusion of redundancy. We also conduct qualitative ablation studies of the ReAtten module using visualization. As shown in (c), in the ViT model without ReAtten, the attention patterns across different sub-images appear extremely fragmented. In contrast, the ViT model with ReAtten shows continuous attention patterns, indicating effective information interaction between sub-images.

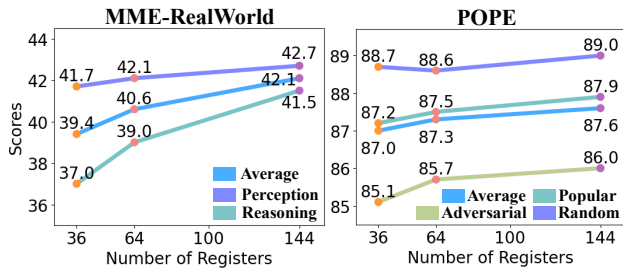


Figure 6. Ablation on different visual register counts. Increasing the number of visual registers generally enhances accuracy across both benchmarks. However, the improvement rate noticeably tapers off when the register count exceeds 64. Based on this observation, to better balance the efficiency and performance, we select register counts of 64 and 36 for FALCON-7B and 3B, respectively.

addressing the issue of visual fragmentation. In contrast, we argue that the information exchange in W-Atten is limited to a local window, which hinders sufficient information exchange among all sub-images. Meanwhile, CIP introduces further redundancy by repeatedly encoding the same visual content, which can even lead to a decline in performance.

Ablation on the Number of Visual Registers. To investigate the impact of changing the number of visual registers on model performance, we conduct experiments with visual register counts set to 36, 64, and 144. These counts correspond to visual token compression rates of $16\times$, $9\times$, and $4\times$, respectively. As shown in Fig. 6, increasing the number of visual registers generally enhances the model’s high-resolution comprehension capabilities and helps reduce hallucinations. However, when the register count exceeds 64, the improvement gains start tapering off noticeably. Meanwhile, increasing visual registers also demands more computational resources. Compared to the baseline model with

36 registers, models configured with 64 and 144 registers require 1.15 and 2.41 times more training time, respectively. Based on these observations, to achieve a better balance between efficiency and performance, we select 64 and 36 as the register counts for FALCON-7B and 3B, respectively.

4.3. Qualitative Analysis

Visualization and Analysis of Attention Maps. To qualitatively analyze the proposed visual register technique, we visualize the register-to-image attention maps within ViT. Specifically, for a particular visual register, we extract the attention scores that this register assigns to image tokens in each sub-image. We then concatenate these attention scores across all sub-images, create a heatmap, and overlay it onto the input image. As shown in Fig. 5(b), each visual register focuses on relatively distinct areas of the image, highlighting that it captures a diverse range of visual details. Moreover, the visual registers tend to avoid background areas in the image, indicating their effectiveness in identifying and discarding visual redundancy. These properties enable visual registers to effectively produce a comprehensive and non-redundant visual representation. Additionally, to qualitatively evaluate the effectiveness of the ReAtten module, we visualize the attention maps of several particular registers within ViT models with and without ReAtten. As shown in Fig. 5(c), in the ViT model without ReAtten, the attention patterns across different sub-images appear highly fragmented. In contrast, the ViT model with ReAtten exhibits continuous attention patterns, indicating effective information exchange between sub-images.

Case Study on Diverse Tasks. As shown in Fig. 7 and Fig. 8, we depict various examples to qualitatively validate the advanced high-resolution understanding abil-

OCR in the Wild (2250×1500)



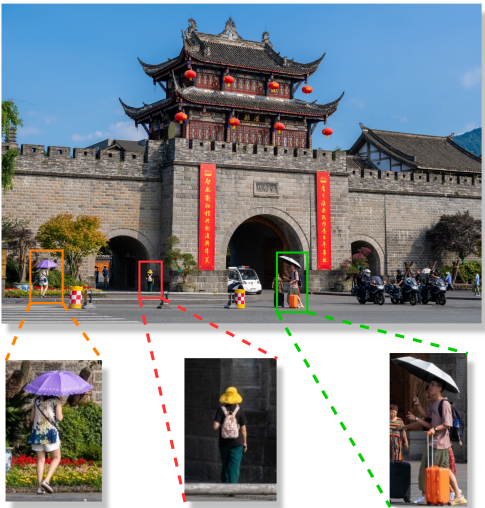
Tell me the number on the traffic light. 

 19

Tell me the full text shown on the blue sign post. 

 The full text on the blue sign post is "Taipei City Hall" in both English and Chinese.

Small Object Dection (2250×1500)



Is the orange luggage on the left or right side of the purple umbrella? 

 Right.

Give the detailed location of the person wearing a yellow hat. 

 The person wearing a yellow hat is standing near the entrance of the building, which is the archway. They are positioned on the left side of the archway, slightly in front of the entrance.

Figure 7. Qualitative analysis of FALCON in high-resolution images of natural scenes. The examples illustrate FALCON’s exceptional capabilities in detecting small objects and recognizing small text in natural scenes, demonstrating its ability to capture rich fine-grained information in high-resolution images.

ities of FALCON. Fig. 7 illustrates FALCON’s exceptional ability to recognize small objects and text in natural scenes, demonstrating its capability to capture rich, fine-grained details in high-resolution images. Furthermore, Fig. 8 highlights FALCON’s proficiency in understanding and summarizing high-resolution document images with dense text, while also demonstrating its sensitivity to small text elements. These examples demonstrate FALCON’s remarkable capabilities across various high-resolution vision-language tasks.

5. Conclusion

To address the visual redundancy and fragmentation in high-resolution MLLMs, we propose FALCON. FALCON employs an innovative visual register technique that simultaneously addresses both challenges. This technique uses a ReCompact mechanism to adaptively aggregate essential visual information through visual registers, creating a compact, non-redundant representation. Additionally, a novel ReAtten module is introduced to facilitate in-

Document Understanding
(1600×1822)

What is Nano?

Nanotechnology - the modern technology of working with substances at the level of individual atoms

What is Nano?
Nanotechnology - the modern technology of working with substances at the level of individual atoms

Types of nanotechnologies:

Top-down approaches - nanoparticles created by splitting larger substance

Bottom-up approaches - building materials from molecular components

Types of nanotechnologies:

Top-down approaches - nanoparticles created by splitting larger substance

Bottom-up approaches - building materials from molecular components

Investments in nanotechnology

Region	Investment Percentage
European Union	27%
USA	19%
Russia	22%
China	10%
Taiwan	2%
Republic of Korea	4%
Japan	12%
Rest of the world	4%

The total volume of state investment in nanotechnology in 2009 is estimated at \$9.75 billion

Investments in nanotechnology

Region	Investment Percentage
European Union	27%
USA	19%
Russia	22%
China	10%
Taiwan	2%
Republic of Korea	4%
Japan	12%
Rest of the world	4%

The total volume of state investment in nanotechnology in 2009 is estimated at \$9.75 billion

RIANOVOSTI © 2010

Describe the image in detail.

The image is a vibrant infographic that provides an overview of nanotechnology. It's divided into three distinct sections, each highlighting a different aspect of this fascinating field.

In the top section, the title "What is Nanotechnology?" is prominently displayed, setting the stage for the information that follows. This section introduces the concept of nanotechnology, explaining that it's the modern technology of working with substances at the level of individual atoms.

The middle section is titled "Types of Nanotechnology", providing a detailed explanation of the different types of nanotechnology. It mentions large-scale nanotechnology, which involves the creation of substances by splitting larger particles into smaller ones, and bottom-up approaches, which involve building materials from molecular components.

The bottom section is titled "Investments in Nanotechnology", detailing the investments made in nanotechnology in various regions of the world. It mentions the USA, Europe, China, Taiwan, Korea, and Japan, each represented by a color-coded bar. The bars indicate the percentage of investment in nanotechnology in each region.

The infographic is a colorful mix of blue, green, orange, and pink, with each color representing a different aspect of nanotechnology. The text is clear and easy to read, making the information accessible to a wide audience. The infographic is a great visual representation of the exciting world of nanotechnology.

Who owns the copyright of this image?

RIANOVOSTI

Figure 8. Qualitative analysis of FALCON in high-resolution images of documents. The example demonstrates FALCON's strong understanding and summarization capabilities for text-intensive, high-resolution document images. It also shows FALCON's ability to recognize small text. This proves FALCON's robustness in capturing rich, fine-grained information across different types of high-resolution images.

formation exchange among sub-images via visual registers, thereby enhancing visual continuity during encoding. Extensive experiments demonstrate FALCON’s superiority in high-resolution understanding and validate the effectiveness of the proposed ReCompact and ReAtten.

References

- [1] Meta AI. Llama 3.2: Revolutionizing edge ai and vision with open, customizable models, 2024. 1
- [2] Jinze Bai, Shuai Bai, Shusheng Yang, Shijie Wang, Sinan Tan, Peng Wang, Junyang Lin, Chang Zhou, and Jingren Zhou. Qwen-vl: A versatile vision-language model for understanding, localization, text reading, and beyond. *arXiv preprint arXiv:2308.12966*, 1(2):3, 2023. 2, 3, 4, 6, 7
- [3] Gongwei Chen, Leyang Shen, Rui Shao, Xiang Deng, and Liqiang Nie. Lion: Empowering multimodal large language model with dual-level visual knowledge. In *Proceedings of the IEEE/CVF Conference on Computer Vision and Pattern Recognition*, pages 26540–26550, 2024. 1, 2
- [4] Guiming Hardy Chen, Shunian Chen, Ruifei Zhang, Junying Chen, Xiangbo Wu, Zhiyi Zhang, Zhihong Chen, Jianquan Li, Xiang Wan, and Benyou Wang. Allava: Harnessing gpt4v-synthesized data for a lite vision-language model. *arXiv preprint arXiv:2402.11684*, 2024. 1
- [5] Jun Chen, Deyao Zhu, Xiaoqian Shen, Xiang Li, Zechun Liu, Pengchuan Zhang, Raghuraman Krishnamoorthi, Vikas Chandra, Yunyang Xiong, and Mohamed Elhoseiny. Minigt-v2: large language model as a unified interface for vision-language multi-task learning. *arXiv preprint arXiv:2310.09478*, 2023. 6
- [6] Lin Chen, Jinsong Li, Xiaoyi Dong, Pan Zhang, Conghui He, Jiaqi Wang, Feng Zhao, and Dahua Lin. Sharegpt4v: Improving large multi-modal models with better captions. *CoRR*, abs/2311.12793, 2023. 6, 1
- [7] Wei-Lin Chiang, Zhuohan Li, Zi Lin, Ying Sheng, Zhanghao Wu, Hao Zhang, Lianmin Zheng, Siyuan Zhuang, Yonghao Zhuang, Joseph E Gonzalez, et al. Vicuna: An open-source chatbot impressing gpt-4 with 90%* chatgpt quality. See <https://vicuna.lmsys.org> (accessed 14 April 2023), 2(3):6, 2023. 2, 1
- [8] Wenliang Dai, Junnan Li, Dongxu Li, Anthony Tiong, Junqi Zhao, Weisheng Wang, Boyang Li, Pascale Fung, and Steven Hoi. InstructBLIP: Towards general-purpose vision-language models with instruction tuning. In *Thirty-seventh Conference on Neural Information Processing Systems*, 2023. 1, 2, 4, 7
- [9] Timothée Darcet, Maxime Oquab, Julien Mairal, and Piotr Bojanowski. Vision transformers need registers. In *The Twelfth International Conference on Learning Representations*, 2024. 3, 4
- [10] Alexey Dosovitskiy, Lucas Beyer, Alexander Kolesnikov, Dirk Weissenborn, Xiaohua Zhai, Thomas Unterthiner, Mostafa Dehghani, Matthias Minderer, Georg Heigold, Sylvain Gelly, Jakob Uszkoreit, and Neil Houlsby. An image is worth 16x16 words: Transformers for image recognition at scale. In *International Conference on Learning Representations*, 2021. 3
- [11] Yash Goyal, Tejas Khot, Douglas Summers-Stay, Dhruv Batra, and Devi Parikh. Making the v in vqa matter: Elevating the role of image understanding in visual question answering. In *Proceedings of the IEEE conference on computer vision and pattern recognition*, pages 6904–6913, 2017. 1
- [12] Dan Hendrycks and Kevin Gimpel. Bridging nonlinearities and stochastic regularizers with gaussian error linear units. *arXiv preprint arXiv:1606.08415*, 2016. 1
- [13] Wenyi Hong, Weihan Wang, Ming Ding, Wenmeng Yu, Qingsong Lv, Yan Wang, Yean Cheng, Shiyu Huang, Junhui Ji, Zhao Xue, et al. Cogvlm2: Visual language models for image and video understanding. *arXiv preprint arXiv:2408.16500*, 2024. 6
- [14] Anwen Hu, Haiyang Xu, Jiabo Ye, Ming Yan, Liang Zhang, Bo Zhang, Chen Li, Ji Zhang, Qin Jin, Fei Huang, et al. mplug-docowl 1.5: Unified structure learning for ocr-free document understanding. *arXiv preprint arXiv:2403.12895*, 2024. 1, 2, 3, 6
- [15] Edward J Hu, yelong shen, Phillip Wallis, Zeyuan Allen-Zhu, Yuanzhi Li, Shean Wang, Lu Wang, and Weizhu Chen. LoRA: Low-rank adaptation of large language models. In *International Conference on Learning Representations*, 2022. 1
- [16] Mingxin Huang, Yuliang Liu, Dingkan Liang, Lianwen Jin, and Xiang Bai. Mini-monkey: Alleviate the sawtooth effect by multi-scale adaptive cropping. *arXiv preprint arXiv:2408.02034*, 2024. 3, 7, 2
- [17] Runhui Huang, Xinpeng Ding, Chunwei Wang, Jianhua Han, Yulong Liu, Hengshuang Zhao, Hang Xu, Lu Hou, Wei Zhang, and Xiaodan Liang. Hires-llava: Restoring fragmentation input in high-resolution large vision-language models. *arXiv preprint arXiv:2407.08706*, 2024. 1, 2
- [18] Drew A Hudson and Christopher D Manning. Gqa: A new dataset for real-world visual reasoning and compositional question answering. In *Proceedings of the IEEE/CVF conference on computer vision and pattern recognition*, pages 6700–6709, 2019. 1
- [19] Sahar Kazemzadeh, Vicente Ordonez, Mark Matten, and Tamara Berg. Referitgame: Referring to objects in photographs of natural scenes. In *Proceedings of the 2014 conference on empirical methods in natural language processing (EMNLP)*, pages 787–798, 2014. 1
- [20] Aniruddha Kembhavi, Mike Salvato, Eric Kolve, Minjoon Seo, Hannaneh Hajishirzi, and Ali Farhadi. A diagram is worth a dozen images. In *14th European Conference on Computer Vision, ECCV 2016*, pages 235–251. Springer Verlag, 2016. 1
- [21] Geewook Kim, Teakgyu Hong, Moonbin Yim, JeongYeon Nam, Jinyoung Park, Jinyeong Yim, Wonseok Hwang, Sangdoon Yun, Dongyoon Han, and Seunghyun Park. Ocr-free document understanding transformer. In *European Conference on Computer Vision (ECCV)*, 2022. 1
- [22] Ranjay Krishna, Yuke Zhu, Oliver Groth, Justin Johnson, Kenji Hata, Joshua Kravitz, Stephanie Chen, Yannis Kalantidis, Li-Jia Li, David A Shamma, et al. Visual genome: Connecting language and vision using crowdsourced dense image annotations. *International journal of computer vision*, 123:32–73, 2017. 1

- [23] Junnan Li, Dongxu Li, Silvio Savarese, and Steven Hoi. Blip-2: Bootstrapping language-image pre-training with frozen image encoders and large language models. In *International conference on machine learning*, pages 19730–19742. PMLR, 2023. 4
- [24] Junyan Li, Delin Chen, Tianle Cai, Peihao Chen, Yining Hong, Zhenfang Chen, Yikang Shen, and Chuang Gan. Flex-attention for efficient high-resolution vision-language models, 2024. 7
- [25] Yifan Li, Yifan Du, Kun Zhou, Jinpeng Wang, Xin Zhao, and Ji-Rong Wen. Evaluating object hallucination in large vision-language models. In *The 2023 Conference on Empirical Methods in Natural Language Processing*, 2023. 6
- [26] Yanwei Li, Yuechen Zhang, Chengyao Wang, Zhisheng Zhong, Yixin Chen, Ruihang Chu, Shaoteng Liu, and Jiaya Jia. Mini-gemini: Mining the potential of multi-modality vision language models. *arXiv preprint arXiv:2403.18814*, 2024. 6
- [27] Zaijing Li, Yuquan Xie, Rui Shao, Gongwei Chen, Dongmei Jiang, and Liqiang Nie. Optimus-1: Hybrid multimodal memory empowered agents excel in long-horizon tasks. In *Advances in neural information processing systems*, 2024. 2
- [28] Zhang Li, Biao Yang, Qiang Liu, Zhiyin Ma, Shuo Zhang, Jingxu Yang, Yabo Sun, Yuliang Liu, and Xiang Bai. Monkey: Image resolution and text label are important things for large multi-modal models. In *Proceedings of the IEEE/CVF Conference on Computer Vision and Pattern Recognition*, pages 26763–26773, 2024. 2, 3, 4, 6, 7
- [29] Haotian Liu, Chunyuan Li, Yuheng Li, and Yong Jae Lee. Improved baselines with visual instruction tuning. In *Proceedings of the IEEE/CVF Conference on Computer Vision and Pattern Recognition*, pages 26296–26306, 2024. 1, 2, 6
- [30] Haotian Liu, Chunyuan Li, Yuheng Li, Bo Li, Yuanhan Zhang, Sheng Shen, and Yong Jae Lee. Llava-next: Improved reasoning, ocr, and world knowledge, 2024. 6, 7
- [31] Haotian Liu, Chunyuan Li, Qingyang Wu, and Yong Jae Lee. Visual instruction tuning. *Advances in neural information processing systems*, 36, 2024. 1, 2, 7
- [32] Yuliang Liu, Biao Yang, Qiang Liu, Zhang Li, Zhiyin Ma, Shuo Zhang, and Xiang Bai. Textmonkey: An ocr-free large multimodal model for understanding document. *arXiv preprint arXiv:2403.04473*, 2024. 1, 2, 3, 4, 6, 7
- [33] Yuan Liu, Haodong Duan, Yuanhan Zhang, Bo Li, Songyang Zhang, Wangbo Zhao, Yike Yuan, Jiaqi Wang, Conghui He, Ziwei Liu, et al. Mmbench: Is your multi-modal model an all-around player? In *European Conference on Computer Vision*, pages 216–233. Springer, 2025. 6
- [34] Ze Liu, Yutong Lin, Yue Cao, Han Hu, Yixuan Wei, Zheng Zhang, Stephen Lin, and Baining Guo. Swin transformer: Hierarchical vision transformer using shifted windows. In *Proceedings of the IEEE/CVF international conference on computer vision*, pages 10012–10022, 2021. 3, 7, 2
- [35] Haoyu Lu, Wen Liu, Bo Zhang, Bingxuan Wang, Kai Dong, Bo Liu, Jingxiang Sun, Tongzheng Ren, Zhuoshu Li, Yaofeng Sun, et al. Deepseek-vl: towards real-world vision-language understanding. *arXiv preprint arXiv:2403.05525*, 2024. 2, 3, 6
- [36] Pan Lu, Liang Qiu, Jiaqi Chen, Tony Xia, Yizhou Zhao, Wei Zhang, Zhou Yu, Xiaodan Liang, and Song-Chun Zhu. Iconqa: A new benchmark for abstract diagram understanding and visual language reasoning. In *Thirty-fifth Conference on Neural Information Processing Systems Datasets and Benchmarks Track (Round 2)*, 2021. 1
- [37] Pan Lu, Swaroop Mishra, Tony Xia, Liang Qiu, Kai-Wei Chang, Song-Chun Zhu, Oyvind Tafjord, Peter Clark, and Ashwin Kalyan. Learn to explain: Multimodal reasoning via thought chains for science question answering. In *The 36th Conference on Neural Information Processing Systems (NeurIPS)*, 2022. 6, 1
- [38] Gen Luo, Yiyi Zhou, Yuxin Zhang, Xiawu Zheng, Xiaoshuai Sun, and Rongrong Ji. Feast your eyes: Mixture-of-resolution adaptation for multimodal large language models. *arXiv preprint arXiv:2403.03003*, 2024. 2
- [39] Kenneth Marino, Mohammad Rastegari, Ali Farhadi, and Roozbeh Mottaghi. Ok-vqa: A visual question answering benchmark requiring external knowledge. In *Proceedings of the IEEE/cvf conference on computer vision and pattern recognition*, pages 3195–3204, 2019. 1
- [40] Ahmed Masry, Xuan Long Do, Jia Qing Tan, Shafiq Joty, and Enamul Hoque. Chartqa: A benchmark for question answering about charts with visual and logical reasoning. In *Findings of the Association for Computational Linguistics: ACL 2022*, pages 2263–2279, 2022. 1
- [41] Minesh Mathew, Dimosthenis Karatzas, and CV Jawahar. Docvqa: A dataset for vqa on document images. In *Proceedings of the IEEE/CVF winter conference on applications of computer vision*, pages 2200–2209, 2021. 6, 1
- [42] Minesh Mathew, Viraj Bagal, Rubèn Tito, Dimosthenis Karatzas, Ernest Valveny, and CV Jawahar. Infographicvqa. In *Proceedings of the IEEE/CVF Winter Conference on Applications of Computer Vision*, pages 1697–1706, 2022. 1
- [43] Anand Mishra, Shashank Shekhar, Ajeet Kumar Singh, and Anirban Chakraborty. Ocr-vqa: Visual question answering by reading text in images. In *2019 international conference on document analysis and recognition (ICDAR)*, pages 947–952. IEEE, 2019. 1
- [44] Panupong Pasupat and Percy Liang. Compositional semantic parsing on semi-structured tables. In *Proceedings of the 53rd Annual Meeting of the Association for Computational Linguistics and the 7th International Joint Conference on Natural Language Processing (Volume 1: Long Papers)*, pages 1470–1480, 2015. 1
- [45] Alec Radford, Jong Wook Kim, Chris Hallacy, Aditya Ramesh, Gabriel Goh, Sandhini Agarwal, Girish Sastry, Amanda Askell, Pamela Mishkin, Jack Clark, et al. Learning transferable visual models from natural language supervision. In *International conference on machine learning*, pages 8748–8763. PMLR, 2021. 2, 3, 1
- [46] Dustin Schwenk, Apoorv Khandelwal, Christopher Clark, Kenneth Marino, and Roozbeh Mottaghi. A-okvqa: A benchmark for visual question answering using world knowledge. In *European Conference on Computer Vision*, pages 146–162, 2022. 1
- [47] Leyang Shen, Gongwei Chen, Rui Shao, Weili Guan, and Liqiang Nie. Mome: Mixture of multimodal experts for gen-

- eralist multimodal large language models. In *Advances in neural information processing systems*, 2024. 2
- [48] Baifeng Shi, Ziyang Wu, Maolin Mao, Xin Wang, and Trevor Darrell. When do we not need larger vision models? *arXiv preprint arXiv:2403.13043*, 2024. 2, 3, 7
- [49] Oleksii Sidorov, Ronghang Hu, Marcus Rohrbach, and Amanpreet Singh. Textcaps: a dataset for image captioning with reading comprehension. In *Computer Vision—ECCV 2020: 16th European Conference, Glasgow, UK, August 23–28, 2020, Proceedings, Part II 16*, pages 742–758. Springer, 2020. 1
- [50] Amanpreet Singh, Vivek Natarajan, Meet Shah, Yu Jiang, Xinlei Chen, Dhruv Batra, Devi Parikh, and Marcus Rohrbach. Towards vqa models that can read. In *Proceedings of the IEEE/CVF conference on computer vision and pattern recognition*, pages 8317–8326, 2019. 6, 1
- [51] S Svetlichnaya. Deepform: Understand structured documents at scale. 2020. 1
- [52] Ryota Tanaka, Kyosuke Nishida, and Sen Yoshida. Visualmrc: Machine reading comprehension on document images. In *Proceedings of the AAAI Conference on Artificial Intelligence*, pages 13878–13888, 2021. 1
- [53] Gemini Team, Rohan Anil, Sebastian Borgeaud, Jean-Baptiste Alayrac, Jiahui Yu, Radu Soricut, Johan Schalkwyk, Andrew M Dai, Anja Hauth, Katie Millican, et al. Gemini: a family of highly capable multimodal models. *arXiv preprint arXiv:2312.11805*, 2023. 6
- [54] Shengbang Tong, Ellis Brown, Penghao Wu, Sanghyun Woo, Manoj Middepogu, Sai Charitha Akula, Jihan Yang, Shusheng Yang, Adithya Iyer, Xichen Pan, et al. Cambrian-1: A fully open, vision-centric exploration of multimodal llms. *CoRR*, 2024. 6
- [55] Hugo Touvron, Thibaut Lavril, Gautier Izacard, Xavier Martinet, Marie-Anne Lachaux, Timothée Lacroix, Baptiste Rozière, Naman Goyal, Eric Hambro, Faisal Azhar, et al. Llama: Open and efficient foundation language models. *arXiv preprint arXiv:2302.13971*, 2023. 2
- [56] Hugo Touvron, Louis Martin, Kevin Stone, Peter Albert, Amjad Almahairi, Yasmine Babaei, Nikolay Bashlykov, Soumya Batra, Prajjwal Bhargava, Shruti Bhosale, et al. Llama 2: Open foundation and fine-tuned chat models. *arXiv preprint arXiv:2307.09288*, 2023. 2
- [57] A Vaswani. Attention is all you need. *Advances in Neural Information Processing Systems*, 2017. 4
- [58] Penghao Wu and Saining Xie. V*: Guided visual search as a core mechanism in multimodal llms. In *Proceedings of the IEEE/CVF Conference on Computer Vision and Pattern Recognition*, pages 13084–13094, 2024. 6
- [59] Zhenhua Xu, Yujia Zhang, Enze Xie, Zhen Zhao, Yong Guo, Kwan-Yee K Wong, Zhenguo Li, and Hengshuang Zhao. Drivegpt4: Interpretable end-to-end autonomous driving via large language model. *IEEE Robotics and Automation Letters*, 2024. 2
- [60] Linli Yao, Lei Li, Shuhuai Ren, Lean Wang, Yuanxin Liu, Xu Sun, and Lu Hou. Deco: Decoupling token compression from semantic abstraction in multimodal large language models. *arXiv preprint arXiv:2405.20985*, 2024. 2, 3, 7
- [61] Yuan Yao, Tianyu Yu, Ao Zhang, Chongyi Wang, Junbo Cui, Hongji Zhu, Tianchi Cai, Haoyu Li, Weilin Zhao, Zhihui He, et al. Minicpm-v: A gpt-4v level mllm on your phone. *arXiv preprint arXiv:2408.01800*, 2024. 6
- [62] Jiabo Ye, Anwen Hu, Haiyang Xu, Qinghao Ye, Ming Yan, Yuhao Dan, Chenlin Zhao, Guohai Xu, Chenliang Li, Junfeng Tian, et al. mplug-docowl: Modularized multimodal large language model for document understanding. *arXiv preprint arXiv:2307.02499*, 2023. 2
- [63] Jiabo Ye, Anwen Hu, Haiyang Xu, Qinghao Ye, Ming Yan, Guohai Xu, Chenliang Li, Junfeng Tian, Qi Qian, Ji Zhang, et al. Ureader: Universal ocr-free visually-situated language understanding with multimodal large language model. In *Findings of the Association for Computational Linguistics: EMNLP 2023*, pages 2841–2858, 2023. 1, 2, 3, 4, 7
- [64] Qinghao Ye, Haiyang Xu, Guohai Xu, Jiabo Ye, Ming Yan, Yiyang Zhou, Junyang Wang, Anwen Hu, Pengcheng Shi, Yaya Shi, et al. mplug-owl: Modularization empowers large language models with multimodality. *arXiv preprint arXiv:2304.14178*, 2023. 1, 2
- [65] Qinghao Ye, Haiyang Xu, Jiabo Ye, Ming Yan, Anwen Hu, Haowei Liu, Qi Qian, Ji Zhang, and Fei Huang. mplug-owl2: Revolutionizing multi-modal large language model with modality collaboration. In *Proceedings of the IEEE/CVF Conference on Computer Vision and Pattern Recognition*, pages 13040–13051, 2024. 1, 2, 3, 4, 7
- [66] Xiaohua Zhai, Basil Mustafa, Alexander Kolesnikov, and Lucas Beyer. Sigmoid loss for language image pre-training. In *Proceedings of the IEEE/CVF International Conference on Computer Vision*, pages 11975–11986, 2023. 2
- [67] Pan Zhang, Xiaoyi Dong, Yuhang Zang, Yuhang Cao, Rui Qian, Lin Chen, Qipeng Guo, Haodong Duan, Bin Wang, Linke Ouyang, et al. Internlm-xcomposer-2.5: A versatile large vision language model supporting long-contextual input and output. *arXiv preprint arXiv:2407.03320*, 2024. 6
- [68] Xiaofeng Zhang, Chen Shen, Xiaosong Yuan, Shaotian Yan, Liang Xie, Wenxiao Wang, Chaochen Gu, Hao Tang, and Jieping Ye. From redundancy to relevance: Enhancing explainability in multimodal large language models. *arXiv preprint arXiv:2406.06579*, 2024. 2
- [69] Yi-Fan Zhang, Qingsong Wen, Chaoyou Fu, Xue Wang, Zhang Zhang, Liang Wang, and Rong Jin. Beyond llava-hd: Diving into high-resolution large multimodal models. *arXiv preprint arXiv:2406.08487*, 2024. 1, 2, 7
- [70] Yi-Fan Zhang, Huanyu Zhang, Haochen Tian, Chaoyou Fu, Shuangqing Zhang, Junfei Wu, Feng Li, Kun Wang, Qingsong Wen, Zhang Zhang, et al. Mme-realworld: Could your multimodal llm challenge high-resolution real-world scenarios that are difficult for humans? *arXiv preprint arXiv:2408.13257*, 2024. 5

FALCON: Resolving Visual Redundancy and Fragmentation in High-resolution Multimodal Large Language Models via Visual Registers

Supplementary Material

A. Implementation Details

A.1. Architecture

We implement FALCON on pretrained LLMs with two different sizes, including Vicuna-v1.5-7B [7] and Llama-3.2-3B-Instruct [1], resulting in FALCON-7B and FALCON-3B, respectively. Both versions employ the pretrained CLIP-ViT-L/14-336px [45] as vision encoder and integrate a two-layer MLP module with GeLU [12] activation to serve as the vision-language projection layer. For FALCON-7B, the number of visual registers is set to 64, while for FALCON-3B, it is set to 36. These settings result in remarkable visual token compression rates of 9x and 16x, respectively. The maximum number of sub-images is set to 16 for both FALCON-7B and FALCON-3B.

A.2. Training Settings

As described in Sec. 3.3, the training process of FALCON involves three stages. In Stage 1, we train only the visual registers and the MLP using the LLaVA-pretrain-558k [29] dataset. The batch size and initial learning rate are set to 256 and 1e-3, respectively, and training is conducted for 1 epoch. In Stage 2, we unfreeze all parameters and train with the ShareGPT4V-PT [6] dataset along with a subset of the DocStruct4M [14] dataset. The combined dataset includes 1.2M image captions and 600K full-text OCR samples. During this stage, we set the batch size to 256 and the initial learning rate to 2e-5, training the model for a single epoch. In Stage 3, we freeze both the vision encoder and the LLM, and fine-tune the LLM with LoRA [15]. The training dataset contains 1M samples collected from publicly available datasets, with details provided in Tab. 5. This stage employs a batch size of 128, with an initial learning rate set to 2e-4 for LoRA parameters and 2e-5 for other trainable parameters. The training is conducted for one epoch. Across all stages, the AdamW optimizer is employed with a weight decay of 0. Additionally, a learning rate warm-up is applied over the initial steps, representing 3% of the total training steps. We utilize four 80GB A800 GPUs for training. The total training time for FALCON-7B and FALCON-3B was approximately 66 hours and 30 hours, respectively.

A.3. Instruction-tuning Datasets

As shown in Tab. 5, we present details of the instruction-tuning dataset used by FALCON in stage 3. This dataset encompasses a diverse range of task types, including dialogue, general VQA, document VQA, grounding, science

Table 5. Instruction-tuning datasets used in stage 3.

Task	Datasets	Size
Dialogue	LLaVA [31], ALLaVA [4], ShareGPT	301K
General VQA	VQAv2 [11], OKVQA [39], A-OKVQA [46], GQA [18]	230K
Document	ChartQA [40], DocVQA [41], TextVQA [50], TextCaps [49], InfoVQA [42], VisualMRC [52], DeepForm [51], OCRVQA [43], WikiTableQuestions [44]	206K
Grounding	RefCOCO [19], Visual Genome [22]	134K
Science	AI2D [20], IconQA [36], ScienceQA [37]	46K
Caption	ShareGPT4V-Cap100K [6]	50K
OCR	SynthDog-en [21]	40K

VQA, caption, and OCR, totaling approximately 1M samples. All data are collected from publicly available dataset.

B. Experimental Details

We perform extensive ablation studies to validate the effectiveness of the proposed ReCompact mechanism and ReAtten module. By default, all ablation experiments use 64 visual registers and up to 9 sub-images. The stage 3 training uses a subset of about 800k samples. The remaining dataset settings and hyperparameters are the same as those described in Appendix A.2.

B.1. Details of the Ablation on ReCompact

Here, we present the implementation details of the ablation study on the ReCompact mechanism. In this study, we remove the visual register and instead use the outputs corresponding to image tokens as the visual representation. We then compress this visual representation through either the pooling module or the Abstractor [65] module before feeding it into the LMM. To ensure fairness, we set the visual token compression rate to $9\times$ for both experiments, aligning with the compression rate used in ReCompact. Specifically, in the pooling module, we applied a 3×3 average pooling layer, followed by a two-layer MLP. For the Abstractor, we set the number of query tokens to 64, while keeping

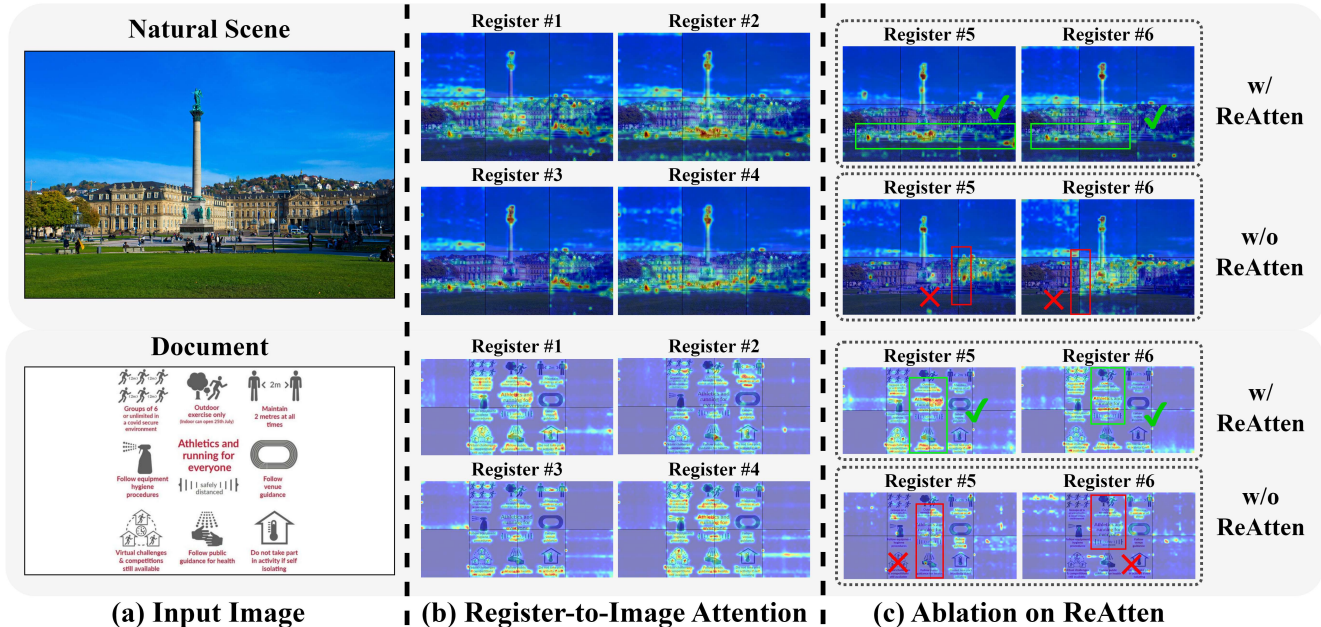


Figure 9. More visualization results of Register-to-Image Attention. The results in (b) demonstrate that ReCompact effectively eliminates redundancy and captures rich visual details across different image types, including natural scenes and documents. The results in (c) further indicate that the ReAtten module ensures continuity in encoding for various image types.

other configurations consistent with mPLUG-Owl2 [65]. All methods are trained using the three-stage pipeline, with the same dataset and training hyperparameters.

B.2. Details of the Ablation on ReAtten

Here we provide implementation details for the ablation study on the ReAtten module. For the Shifted Window Attention (W-Atten) [34] module used in TextMonkey [32], the original design places W-Atten in layers 2, 6, 24, 46 of a 48-layer ViT model. To retain a similar relative depth in the 24-layer CLIP-ViT-L/14 model, we inserted W-Atten in layers 2, 3, 12, 23, respectively. All other configurations are consistent with those in TextMonkey. For the Complementary Image Pyramid (CIP) Strategy proposed by Mini-Monkey [16], to maintain a total maximum sub-image count consistent with other methods (9 sub-images), we set the maximum number of sub-images to 6 for CIP’s detailed group and 3 for the adaptive group, respectively. All methods are trained using the three-stage pipeline, with the same dataset and training hyperparameters. We initialize from the same checkpoint obtained after the stage 2 training. Then, we apply the different methods mentioned above for stage 3 training on the same instruction tuning dataset.

C. More Visualization of Attention Maps

As shown in Fig. 9, we perform further visualization analysis on the models that incorporate the ReCompact and

ReAtten techniques. The results in (b) show that the ReCompact mechanism effectively reduces redundancy while capturing rich visual details across different image types, including natural scenes and documents. The results in (c) further highlight that the ReAtten module maintains continuity in encoding across various image types.

D. Broader Impact and Potential Risk

FALCON employs readily available LLMs, which means it inherently shares some of their limitations. This includes the potential for hallucinating ungrounded text or producing biased results. We mitigate such limitations by performing vision-language instruction tuning on a diverse set of high-quality datasets. Nevertheless, we recommend conducting a thorough investigation into its safety and fairness for the intended use before applying it in practice.